



<https://doi.org/10.31217/p.38.1.12>

# Investigations of Rudder-propeller Clearance on Thrust Performance and Flow Field in Vicinity of Propeller

Sunarsih\*, Aswin Kiftan Ndraha, Achmad Baidowi

Department of Marine Engineering, Faculty of Marine Technology, Institut Teknologi Sepuluh Nopember, Surabaya 60111, Indonesia

\*Corresponding author, e-mail: sunarsihits@gmail.com

---

## ARTICLE INFO

### Original scientific paper

Received 26 April 2024

Accepted 17 June 2024

### Key words:

Propeller clearance  
Rudder position  
Rudder-propeller interaction  
Rudder surface  
Mesh sensitivity  
Sustainable shipping

---

## ABSTRACT

The presence of the propeller affects the hydrodynamics of the rudder in the same way that the ship's hull interferes with the function of the propeller behind and vice versa. Therefore, the arrangement of the propeller and rudder is very important in determining the overall ship propulsion performance. This paper presents a numerical analysis of the KCS propulsion system at various longitudinal clearances with respect to the rudder position. The analysis was performed in a full ship configuration using the KCS hull, propeller, and rudder. The propeller clearance was varied on the basis of the existing KCS design, design adjustments, and recommendations from DNV by 0.124, 0.129, and 0.100 D. Propeller performance was analysed based on individual variations, interactions between the propeller and rudder, and variations in the number of meshes of 0.5, 1.0, and 1.5 mil. The flow distribution around the propeller and the pressure distribution of the rudder inflow onto the rudder surface are also discussed. Numerical examination revealed that DNV's recommended clearance of 0.100 D provided the best results and improved KCS propulsion performance compared with the existing design. The mesh sensitivity analysis revealed that the recommended clearance showed excellent performance in all mesh variations. In response to these findings, modification of the KCS propeller clearance following DNV recommendations would be beneficial to improve overall ship performance.

---

## 1 Introduction

A ship propulsion system greatly governs the overall ship performance. In a full configuration, it involves the steering system governed by the rudder. As a component of the ship system, the interaction among the ship hull, propeller, and rudder is important in defining the overall ship performance. In particular, rudder-propeller interaction affects the total thrust produced by the propeller due to the drag or lift caused by the rudder [1]. In contrast, rudder forces, even in a stationary or slowly moving ship, may be generated by increasing the propeller speed [2].

Among the parameters determining the rudder-propeller interaction is the distance between the two, which is known as propeller clearance. The parameter

that indicates the position of the propeller with respect to the rudder also signifies the propeller distance against the ship hull (hull-propeller clearance). Fig. 1 depicts a detailed measurement of the clearance defined by the classification societies of Det Norske Veritas (DNV) and Lloyds Register (LR).

Normally, rudders are set longitudinally in line with the propeller and located in the propeller slipstream for various reasons, including the increment of propulsive efficiency by taking advantage of the rotational energy in the slipstream. In steady ahead movement, rudder forces in such a setting are typically more than twice those in the outside slipstream arrangement [2]. However, the position of the rudder relative to the propeller may vary in the longitudinal (X), lateral (Y), or vertical (Z) arrangement, as illustrated in Fig. 2 [1].

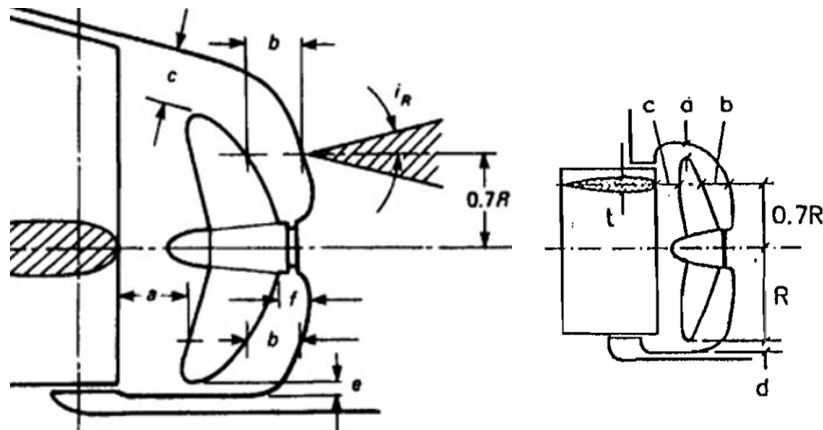


**Figure 1** Propeller clearance by DNV and LR [3,4]

For  $D$  representing the propeller diameter, the only effective variable for a single screw arrangement is the longitudinal clearance of  $X/D$  [1]. DNV recommended a typical value of more than 0.10, whereas LR gave 0.12. A minimum value equals  $t$ , representing the rudder thickness at 0.7  $R$ , as shown in Fig. 1 is advised by the latter. On the other hand, various  $X/D$  values by 0.25 - 0.5 were used in existing ships with some local variations due to the rake and other designs or stern arrangements. The values may also vary in smaller number by 0.1 - 0.24 [5]. Laterally and vertically, the rudder and propeller for this type of arrangement are normally laid to a clearance of  $Y/D = 0$  and  $Z/D = 1.0$ .

Generally, the consideration in taking the value is rather unclear for either propulsion, manoeuvring or other purposes. The basic principle is to provide a suitable clearance to avoid propeller-excited vibration or satisfy the minimum clearance required by the classifications [1]. Despite the dispute, past research in the field displayed the interest towards both objectives and other related performance characteristics such as propeller performance, flow field in the propeller vicinity and hull-rudder-propeller interactions [5-11] to the ex-

tent of the structural response of the rudder in such various stern arrangements [12].

The vagueness in the determination of clearance is clearly shown in the work of [6] and [13]. For the same case study of the ITTC benchmark ship of KCS, the earlier took  $X/D$  values of 0.37, 0.54, 0.63, 0.72, and 0.804, while the latter set a smaller range by 0.54, 0.59, 0.65, 0.71, and 0.76. Either groundless or simply hidden, no clear justifications were exposed as to why such variations were taken into consideration in the studies. In contrast to the earlier work, which employed the ship hull in the analysis, the latter work merely used the propeller and rudder in the setup, creating similar configuration as in recent study by [12].

Exclusion of the ship hull obviously changes the stern hydrodynamic system [14] because of the alteration of the flow field uniformity behind the hull. In return, this affects the hull-rudder-propeller interactions and hence the overall ship performance evaluation. In such consideration, previous studies exploited hull, propeller, and rudder interactions in full configuration [6,8-9]. Analyses were conducted further on the extent of propeller cavitation [15] and manoeuvrability assessment [7] along with the engine and rudder.

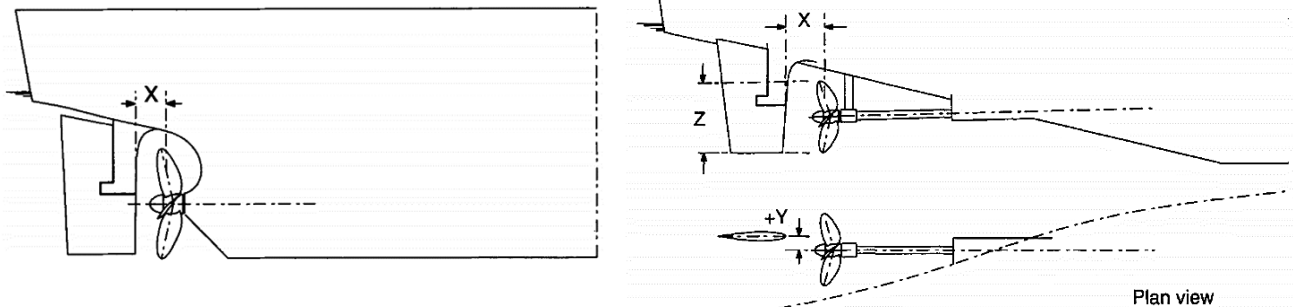


**Figure 2** Propeller clearance for single and twin-screw [1]

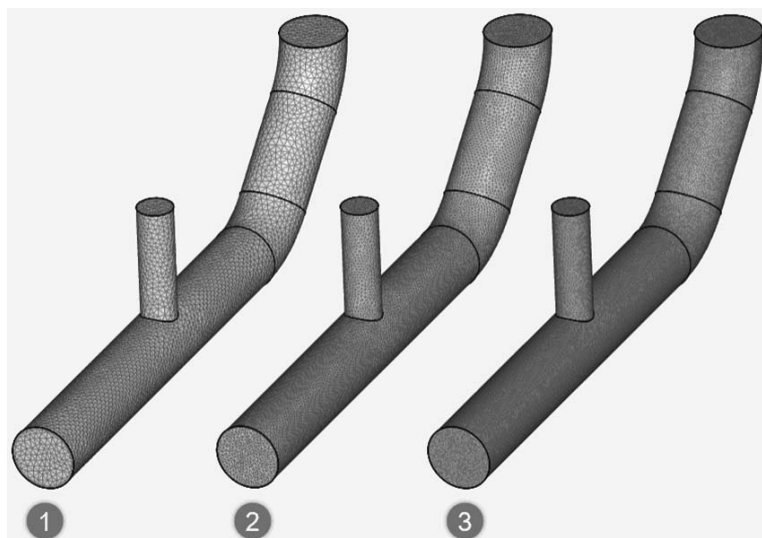


**Figure 3** A set of meshes for sensitivity study: ① 150k cells; ② 300k cells; ③ 600k cells [18]

This paper presents a numerical analysis of the ITTC benchmark KRISO Container Ship (KCS) propulsion system in various longitudinal clearances with respect to the rudder position ( $X/D$ ). The analysis was conducted in a full ship configuration employing a KCS hull, propeller, and rudder. Propeller clearances were varied on the basis of the existing KCS design [16], adjustments to the design, and recommendations addressed by DNV. The study also performed mesh sensitivity analysis in various numbers of cells to ensure the correctness of the modelling and simulations, and hence increase the confidence in the generated solutions.

## 2 Mesh Sensitivity Analysis

Computer modelling and simulation programming have proven the ability to mimic real-world processes and/or problems and provide numerical solutions for the prediction or approximation of processes using the applied algorithms. Evaluation to check and ensure the reliability of this solution is required to increase confidence in using the result. Therefore, the need for verification and validation (V&V) of the simulation is indispensable. Verification examines the correctness of the algorithms in solving the equations in the modelling, while validation evaluates the accuracy of the model to represent real-world applications [17].

Among the best approaches for V&V of computational fluid dynamics (CFD) simulations is mesh sensitivity analysis, which is also known as mesh independence or mesh convergence study [18]. This study involves running a similar simulation configuration using grids of various resolutions, as shown in Fig. 3. Analysis is performed by examining how the converged solutions change with respect to each mesh.

Various studies on mesh sensitivity analysis have been conducted, ranging from structural, mechanics, and materials to marine applications [19-24]. Recently, a study employed a method for measuring the V&V of a full-scale ship against the measured data [25]. In this study, mesh sensitivities involving the number of elements and grid sizes were analysed for various ship powering settings. Generally, the analysis revealed that smaller meshes tend to overestimate the target values.

## 3 Numerical Simulation

### 3.1 Ship and Propeller Particulars

KCS is a 3600 TEU container ship representing a modern ship with a bulbous bow. The ship has a Froude number of 0.26, which corresponds to a service speed of 24 knots. The propeller used is a five-blade right-handed KRISO KP505. Table 1 summarises particulars

**Table 1** Particulars of KCS hull, propeller and rudder

| Ship hull      |         | Propeller         |        | Rudder |                    |
|----------------|---------|-------------------|--------|--------|--------------------|
| LPP            | 230.0 m | Type/Series       | KP-505 | Type   | Semi balanced      |
| B              | 32.2 m  | D                 | 7.9 m  | H      | 9.9 m              |
| T              | 10.8 m  | P/D               | 0.997  | S      | 115 m <sup>2</sup> |
| C <sub>b</sub> | 0.6505  | Ae/A <sub>0</sub> | 0.800  | Z      | 5                  |

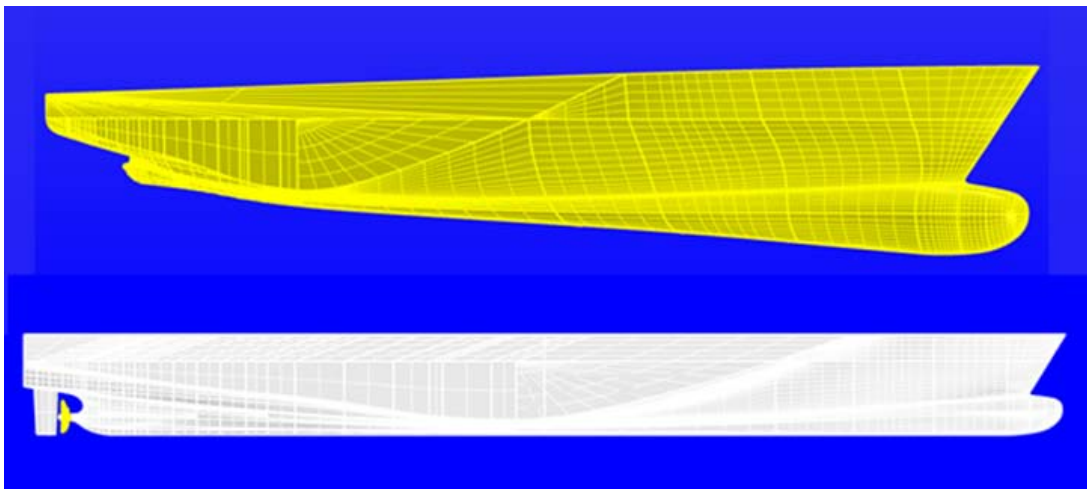


**Figure 4** Bare hull and fully configured KCS

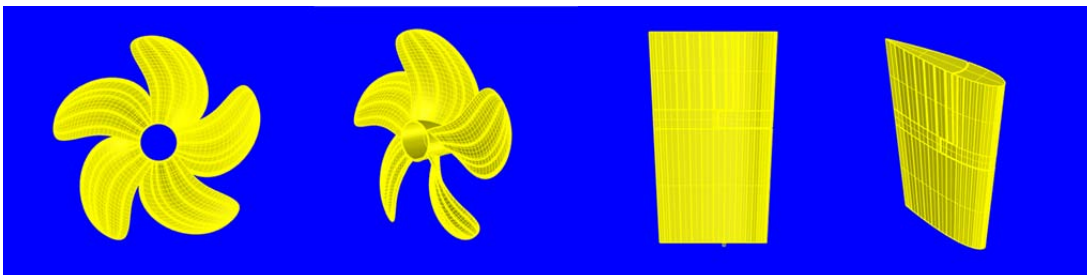


**Figure 5** KCS propeller and rudder model

of the KCS, propeller, and rudder. Fig. 4 and Fig. 5 depict the hull, propeller, and rudder model generated from the particulars, respectively.

### 3.2 Propeller Clearance

The current research investigated three lateral rudder-propeller clearances denoted as X, as tabulated in Table 2. Fig. 6 depicts the KCS stern part which arrangement is to be varied in the clearance.

**Table 2** Propeller clearance for performance evaluation

| X/D   | Distance (mm) | Remarks            |
|-------|---------------|--------------------|
| 0.100 | 790           | DNV recommendation |
| 0.124 | 982           | KCS existing       |
| 0.129 | 1018          | KCS modified       |

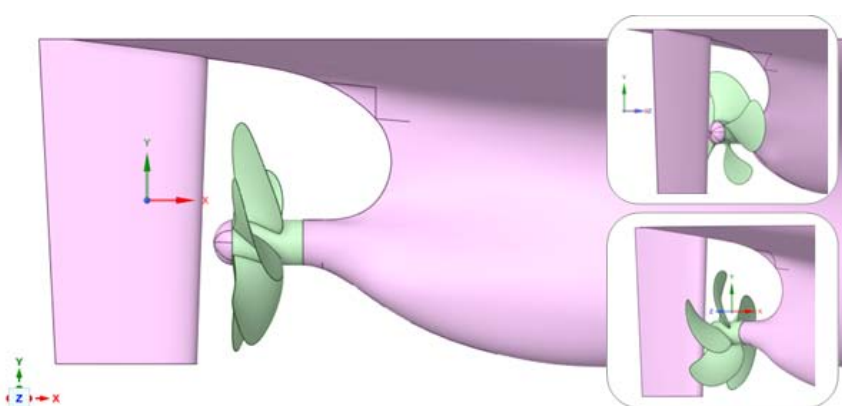


**Figure 6** Stern arrangement of KCS

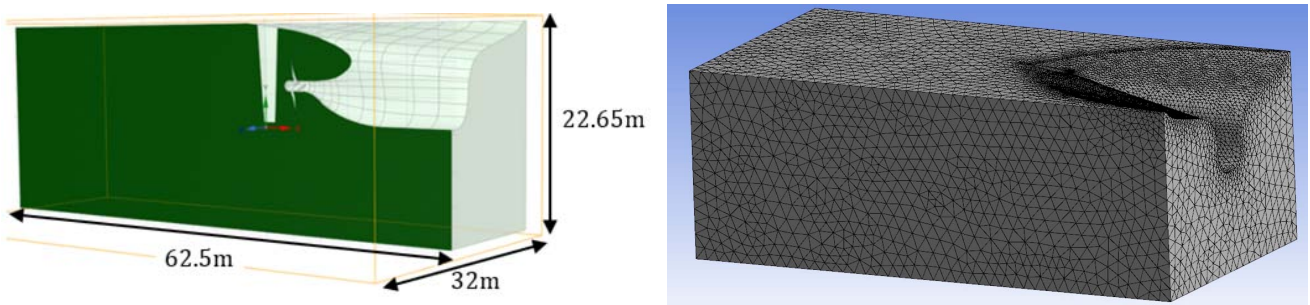


**Figure 7** Model geometry and meshing

### 3.3 Geometry and Meshing

The geometry and meshing of the KCS model are shown in Fig. 7. In the modelling process, the geometry allows checking of the model solidity and creation of the domain and boundary of the test performed, including the fluid characteristics. Subsequently, fractioning the geometry into smaller parts for computation in the meshing stage requires careful consideration. Smaller elements provide more accurate computation results. However, it requires more time and storage because of more computations.

### 3.4 Setup and Solution

The simulation setup was configured for the parameters, fluid properties, and boundary conditions. The computation of a particular test is considered complete once the simulation result (solution) converges. Howev-

er, the level of convergence may vary depending on the availability of sampling resources, such as the cost of CFD simulations [26]. As a more accurate approximation requires more meshing elements and thus more computation, a longer iteration is indispensable to reach convergence. Therefore, careful consideration is required to select the best configuration for a reliable result with reasonable effort and time frame.

### 3.5 Verification

Computer modelling and simulation require verification to check and ensure it free of any faults [18] hence increase the confidence in the simulation results. This study exploited mesh sensitivity analysis by testing all X/D configurations with various mesh numbers. Three meshing variations were selected with 0.5, 1, and 1.5 mil of elements. Meshing profile for each variation is depicted in Fig. 8.

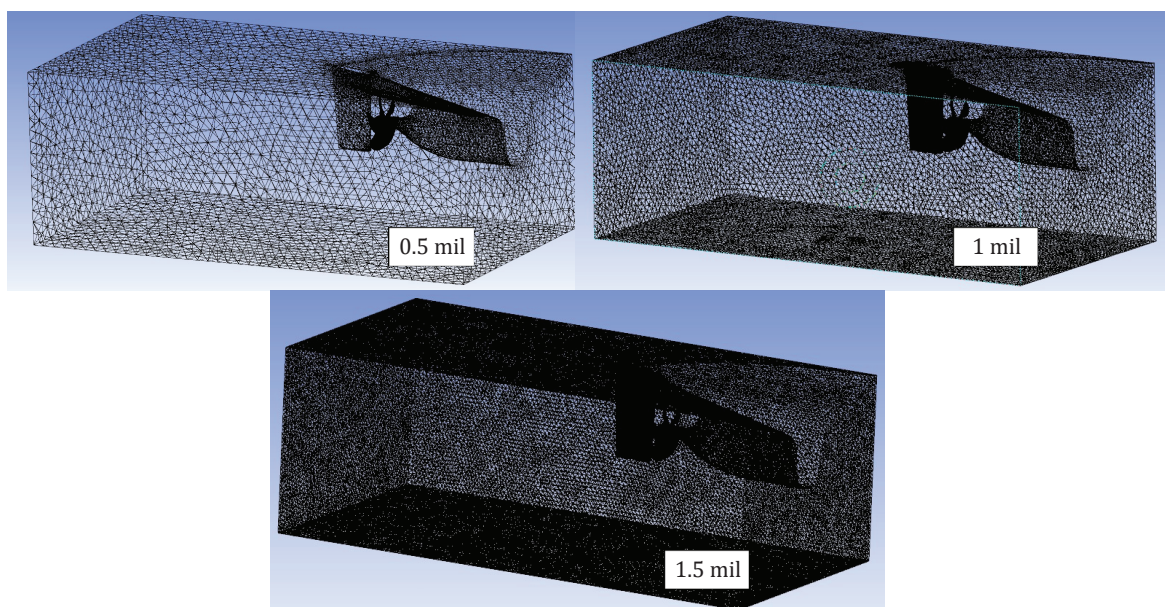


**Figure 8** Meshing profiles for sensitivity analysis

## 4 Result and Discussion

### 4.1 Propeller Performance in Various Rudder-propeller Clearances

The effect of various rudder-propeller clearances on thrust performance is depicted in Fig. 9. In the figure, propeller thrust is profiled for each X/D based on the DNV recommendation (0.100), existing KCS design (0.124), and modification to the design (0.129). The X/D ratios correspond to lateral rudder-propeller distances X of 790, 982, and 1018 mm, respectively.

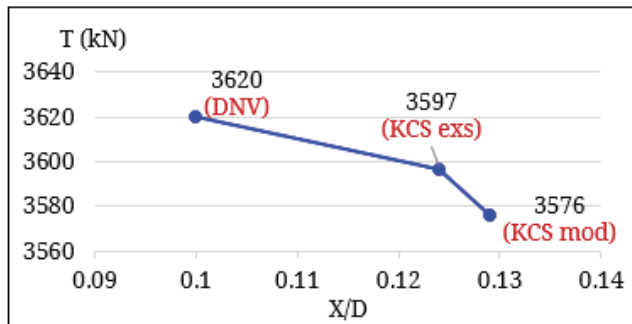


**Figure 9** Propeller thrust at various clearances

As shown in the profile, the larger the rudder-propeller clearance, the lower the thrust generated by the propeller. As the clearance increases, the thrust decreases more rapidly, as indicated by the existing KCS design and the modified profiles. The obtained profiles for the observed clearance conform with the results obtained in previous studies, as depicted in Fig. 10 [5].

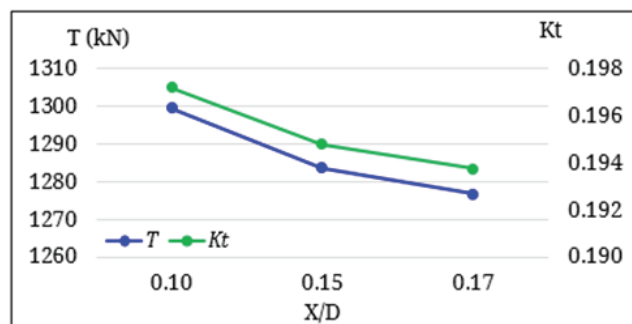


**Figure 10** Propeller thrust at various clearances

Despite the difference in the case studied, this cross validation disclosed a generic behaviour of thrust performance for the observed clearances, i.e. 0.10-0.17 D. As such, it can be generally deduced that the recommendation of the clearance from DNV by 0.100 D is more promising in providing a greater thrust than the LR recommendation by 0.120 D. Obviously, a smaller clearance is out of question except as advised by the classification society.

### 4.2 Flow Field in Vicinity of Propeller

Fig. 11 depicts the stern flow distribution for various rudder-propeller clearances. As observed in the figure, the smallest clearance of X/D = 0.100 by the DNV recommendation developed a higher speed and more regular flow downstream of the rudder, as indicated by the blue arrow. A closer rudder-propeller clearance allows the propeller-induced axial velocity to pass over the distance quicker and creates a higher rudder axial inflow velocity. The more elongated flow downstream of the rudder is expected to build up because of the influence of the rudder tip vortex.

In the larger clearances of 0.124 D and 0.129 D, the flow downstream of the rudder tends to be slower and spread over, which is presumed to be caused by a farther rudder-propeller gap and a smaller rudder tip vortex. Meanwhile, the lowest inflow and flow field in the vicinity of the propeller appear at the greatest clearance of X/D = 0.129, as indicated by the white arrows. These behaviours are believed to occur due to rudder-propeller interaction [1], where the propeller-induced swirl and acceleration in the flow alters the speed and incidence of the flow arriving at the rudder situated aft of the propeller, while the rudder blocks the upstream flow onto and through the propeller, as illustrated in Fig. 12.

Based on the illustration, it is expected that a wider rudder-propeller clearance creates a less blockage effect on the propeller. As the initial clearance of X is widened to a distance of X', the less blockage effect lowers the pressure and speed of the flow upstream of the propeller and accordingly the inflow velocity. In return, the condition affects propeller performance, as indicated by the following expression.

$$T = \frac{1}{J^2} K_T \rho V_a^2 D^2 \quad (1)$$

where

$$K_T (J) = T / \rho n^2 D^4 \quad (2)$$

$$J = V_a / nD \quad (3)$$

Moreover, a wider area between the rudder and propeller provides more space to 'trap' the swirl-containing stream induced by the propeller. The presence of this stream in the area disturbs the function and reduces propeller capability. As such, a smaller clearance allows better propeller performance due to less significant interference from the rudder-propeller interaction. This clarifies propeller performance in various clearances disclosed previously and justifies the best performance of the smallest configuration of X/D = 0.100. As evidenced, the propeller and rudder are interrelated and the interaction affects the thrust produced by the propeller.

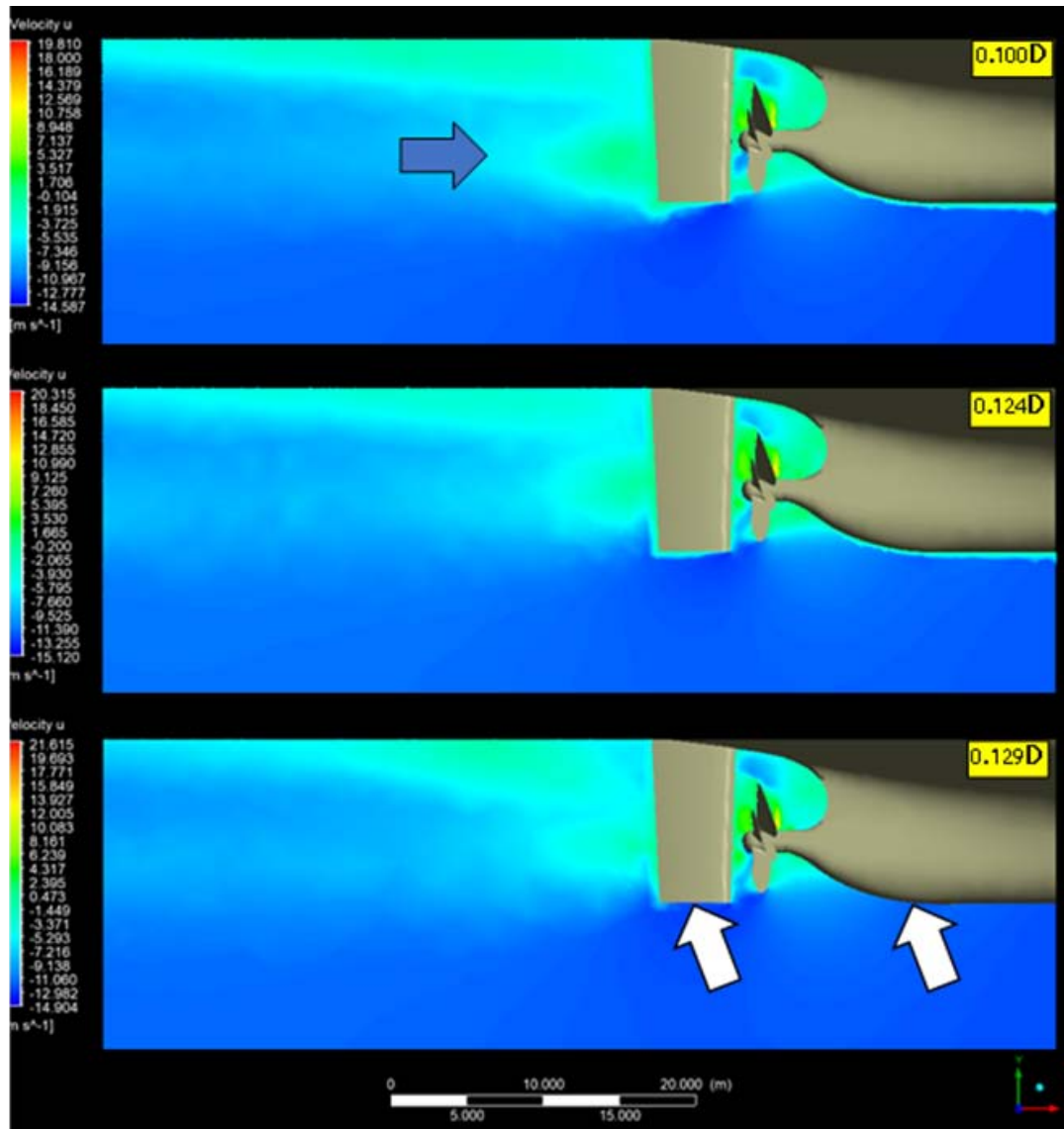


**Figure 11** Axial velocity alongside propeller and rudder

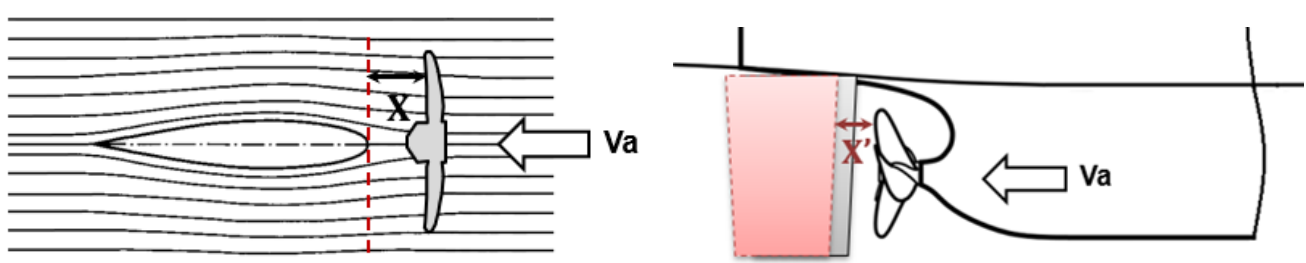


**Figure 12** Blockage effect of rudder on propeller and effect of rudder clearances on inflow velocity

### 4.3 Pressure Distribution on Rudder Surface

Pressure distributions on pressure and suction side of the rudder at various propeller clearances obtained from the simulations are depicted in Fig. 13 and Fig. 14, respectively. In the figures, LE and TE signify the leading and trailing edges of the section. The upper part of the section is referred to as the root, whereas the tip implies the lower part.

It can be seen from the figures that various rudder-propeller clearances induce pressure distribution on the rudder surface differently. On the leading edge, a high-pressure region was formed on both the root and tip of the rudder because of exposure to propeller slip stream hitting the areas continuously during operation. The pressure level on the tip, which tends to be higher than that on the root, is expected because of the hydrostatic pressure originating from these points. Among

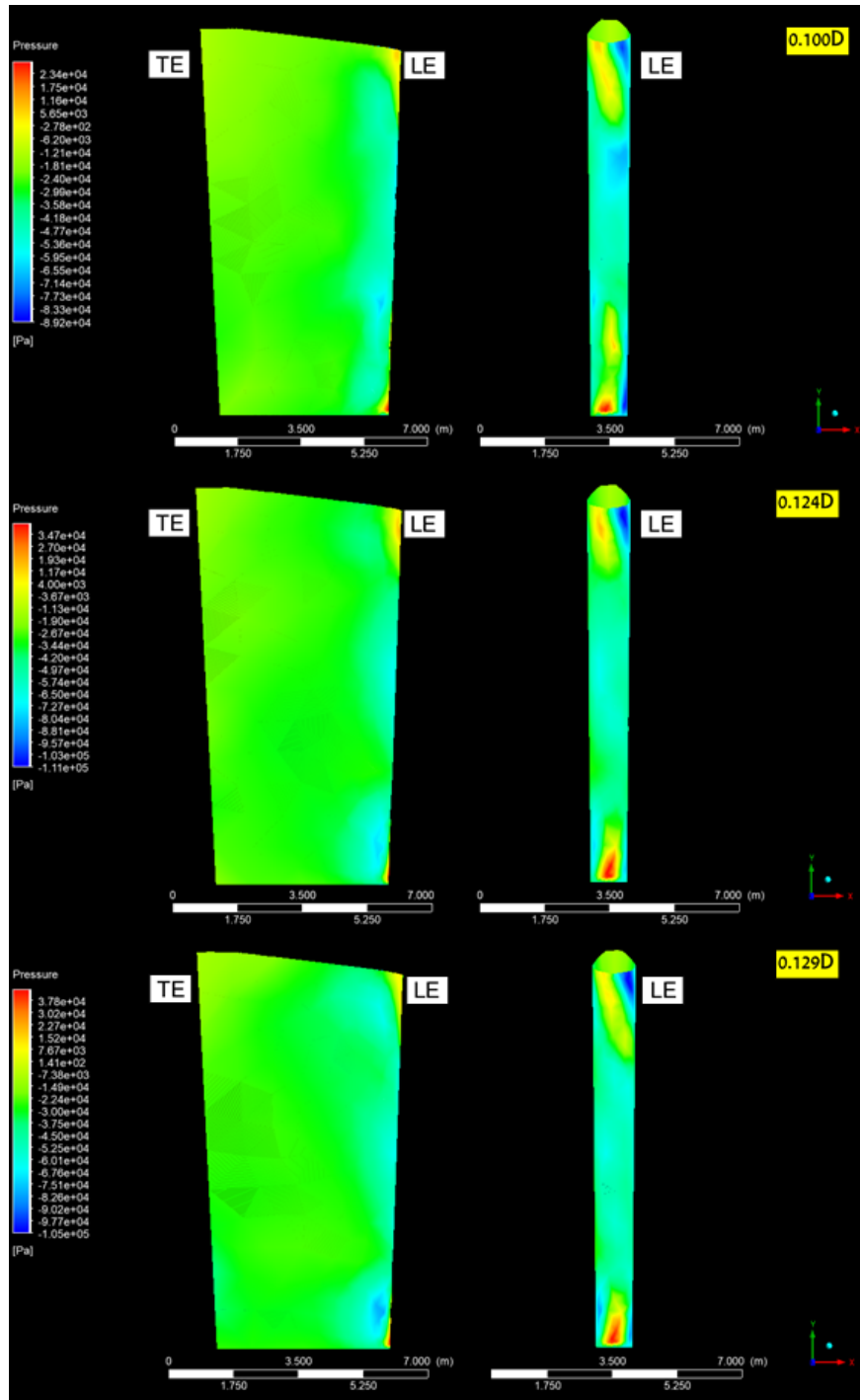


**Figure 13** Pressure distribution on pressure side of the rudder

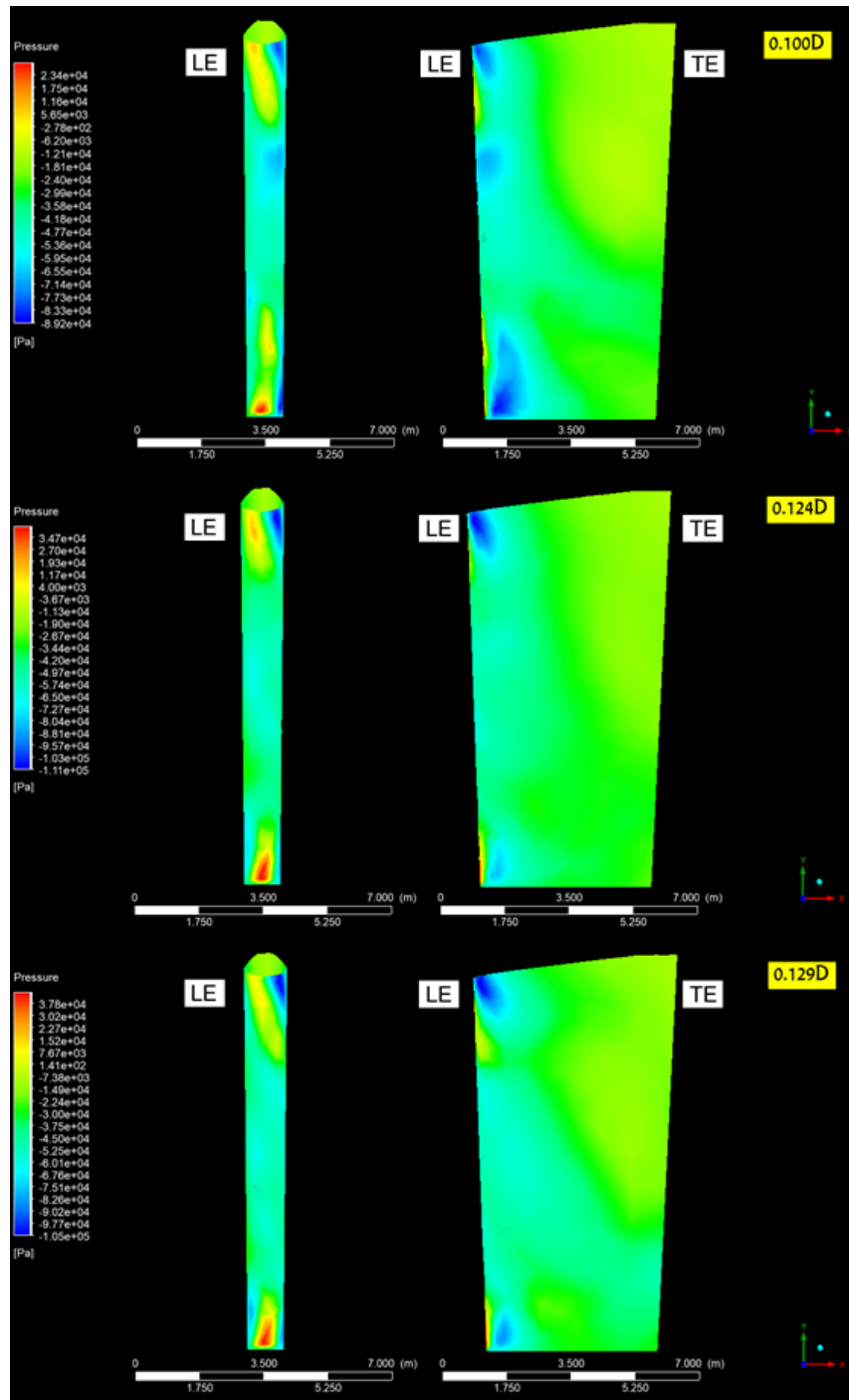


Figure 14 Pressure distribution on suction side of the rudder

the variations, the highest pressure is observed on the tip of the widest clearance of the 0.129 D configuration.

As shown in the figure, a low-pressure region was formed parallel to the high-pressure region on the leading edge of the rudder tip. These high- and low-pressure regions indicate the rudder sides such that the high-pressure region represents the rudder pressure side, whereas the low-pressure region signifies the suction side. As implied and revealed in the figures, the pres-

sure side consistently possesses a higher pressure level than the suction side.

It can also be observed from the figures that there is no significant difference in the pressure sides of all clearance variations. However, several low-pressure regions were formed distinctively on the suction side with the smallest clearance of 0.100 D, particularly on the slipstream area. This phenomenon is expected to occur because of the high acceleration in the down-

stream flow within a smaller area, as discussed previously. As the clearance becomes wider, there is more space to 'trap' and block the stream, which causes the flow to decelerate and hence allows the low pressure to rise gradually. As the clearance becomes wider, the stream decelerates and the low pressure gradually rises because of the wider space, which blocks the propeller stream and accumulates pressure within the space.

#### 4.4 Correctness of Modelling and Simulation

The sensitivity of the mesh number for various rudder-propeller clearance is shown in Fig. 15. Generally, all mesh numbers produce consistent results. As the number of cells increases, the propeller thrust decreases accordingly. This trend conforms with previous research in mesh sensitivity analyses that smaller mesh numbers tend to overestimate the target or average values [19-25], as depicted in Fig. 16 [25]. In fact, a greater mesh number approximates the real condition better and hence provides a more accurate computation.

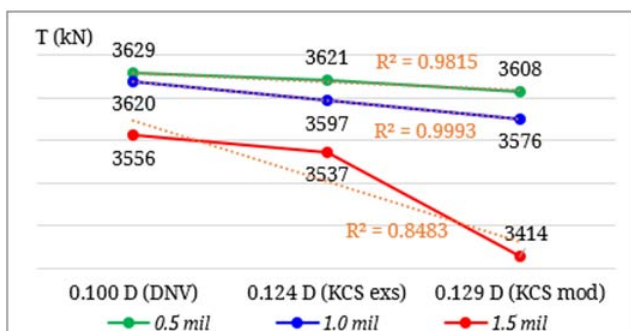


Figure 15 Mesh sensitivity at various rudder-propeller clearances

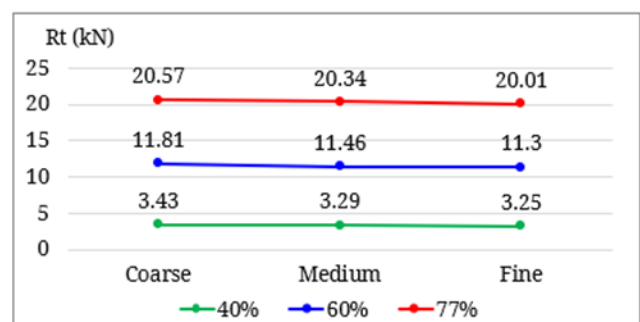


Figure 16 Mesh sensitivity at various ship power ratings

Among the generated solutions a distinct behaviour appeared at 1.5 mil cells for a clearance of 0.129 D, representing the modified KCS design where the propeller thrust produced dropped by 4.95% of the average of two other smaller meshes. This phenomenon is believed to occur because of the large rudder-propeller clearance, as outlined previously. Taking into account the generated solutions for other simulations at 0.5 mil and 1.0 mil cells, the three profiles made up an R-squared ( $R^2$ ) of 0.85 as indicated in the figure. Adopting the statistical approach, as higher  $R^2$  values correlate with lower standard deviation, the difference in the profiles is considered to be insignificant [26]. Moreover, the simulation result for the profile reached the convergence state, as depicted in Fig. 17.

#### 5 Conclusion

For the case of the KCS, the recommended rudder-propeller clearance from DNV by 0.100 D shows better thrust performance than the existing design. The clearance, which is smaller than its original design of  $X/D = 0.124$ , enhances the flow field in the vicinity of the

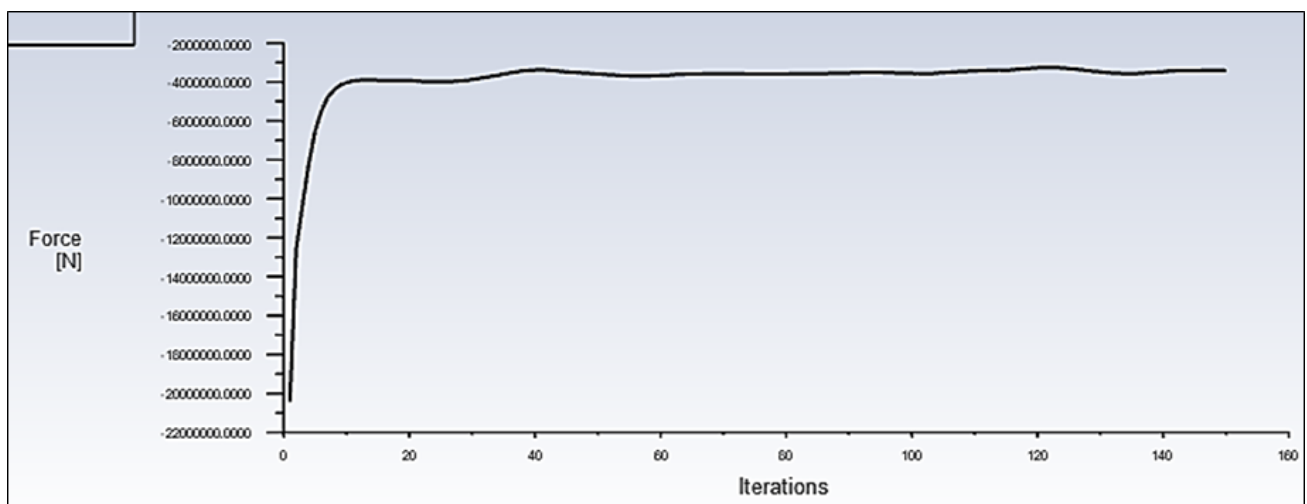


Figure 17 Convergence profile of  $X/D = 0.129$  computation with 1.5 mil cells

propeller and reduces the pressure on the rudder surface located downstream of the propeller. On the contrary, a larger clearance leads the axial velocity in the vicinity of the propeller to rise more rapidly, which results in a reduction in propeller performance and escalates the distribution of pressure on the rudder surface. Simulation of the clearance at various mesh numbers with 0.5 mil, 1.0 mil, and 1.5 mil cells revealed that the clearance persistently excels over larger ones by  $X/D = 0.124$  and  $X/D = 0.129$ . Continuing this success, simulations with the entire ship hull will provide even more promising results. In addition, further investigation into the hull-propeller-rudder interactions in full configuration and how these interactions affect overall ship performance, such as during manoeuvring is also needed, considering that the combination of rudder and propeller governs the side force developed by the ship hull.

**Funding:** The research presented in the manuscript did not receive any external funding.

**Acknowledgment:** The authors gratefully acknowledged financial support from the Institut Teknologi Sepuluh Nopember for this work, under project scheme of the Publication Writing and IPR Incentive Program (PPHKI) 2023.

## References

- [1] Molland, A.F. and Turnock, S.R., 2011. *Marine rudders and control surfaces: principles, data, design and applications*. Elsevier.
- [2] Bertram, V., 2012. *Practical ship hydrodynamics*. Elsevier.
- [3] Schneekluth, H. and Bertram, V., 1998. *Ship design for efficiency and economy* (Vol. 218). Oxford: Butterworth-Heinemann.
- [4] Ghose, J.P., 2004. *Basic ship propulsion*. Allied publishers.
- [5] Jamali, A., 2011. Investigation of propeller characteristics with different locations of the rudder.
- [6] Karim, M.M. and Naz, N., 2017. Computation of flow field around ship hull including self propulsion characteristics at varying rudder positions. *Procedia engineering*, 194, pp. 96-103.
- [7] Oltmann, P. and Sharma, S.D., 1984. *Simulation of combined engine and rudder maneuvers using an improved model of hull-rudder-propeller interactions*.
- [8] Win, Y.N., 2014. *Computation of the Propeller-Hull and Propeller* (Doctoral dissertation, 博士論).
- [9] Guo, H.P., Zou, Z.J., Liu, Y. and Wang, F., 2018. Investigation on hull-rudder-propeller interaction by RANS simulation of captive model tests for a twin-screw ship. *Ocean Engineering*, 162, pp. 259-273.
- [10] Villa, D., Franceschi, A. and Viviani, M., 2020. Numerical analysis of the rudder-propeller interaction. *Journal of Marine Science and Engineering*, 8(12), p. 990.
- [11] Franceschi, A., Piaggio, B., Villa, D. and Viviani, M., 2022. Development and assessment of CFD methods to calculate propeller and hull impact on the rudder inflow for a twin-screw ship. *Applied Ocean Research*, 125, p. 103227.
- [12] Magionesi, F., Dubbioso, G. and Muscari, R., 2022. Contribution of tip and hub vortex to the structural response of a marine rudder in the propeller slipstream. *Journal of Fluid Mechanics*, 946, p. A23.
- [13] Sembiring, H.D.E., Chrismianto, D. and Manik, P., 2016. Pengaruh Jarak Rudder dan Propeller terhadap Kemampuan Thrust menggunakan Metode CFD (Studi Kasus Kapal Kriso Container Ship). *Jurnal Teknik Perkapalan*, 4(1).
- [14] Birk, L., 2019. *Fundamentals of ship hydrodynamics: Fluid mechanics, ship resistance and propulsion*. John Wiley & Sons.
- [15] Regener, P.B., 2016. *Hull-Propeller Interaction and Its Effect on Propeller Cavitation*. DTU Mechanical Engineering.
- [16] NMRI, 2022. *KRISO Container Ship (KCS)*. <https://www.t2015.nmri.go.jp/>. Accessed 1st July 2022.
- [17] Coleman, H.W. and Steele, W.G., 2018. *Experimentation, validation, and uncertainty analysis for engineers*. John Wiley & Sons.
- [18] R. Gasparini. 2022. *Mesh Sensitivity Study for CFD Simulations*. <https://www.simscale.com/>. Accessed 1st July 2022.
- [19] Guo, L., Xiang, J., Latham, J.P. and Izzuddin, B., 2016. A numerical investigation of mesh sensitivity for a new three-dimensional fracture model within the combined finite-discrete element method. *Engineering Fracture Mechanics*, 151, pp. 70-91.
- [20] Kang, J.W. and Lee, J., 2017. Mesh-sensitivity analysis of seismic damage index for reinforced concrete columns.
- [21] AlNajmi, L. and Abed, F., 2020. Evaluation of FRP bars under compression and their performance in RC columns. *Materials*, 13(20), p. 4541.
- [22] Daricik, F., 2019. Mesh size sensitivity analysis for interlaminar fracture of the fiber-reinforced laminated composites. *Journal of Engineered Fibers and Fabrics*, 14, p. 1558925019883460.
- [23] Nurrahman, R., Shuib, A., Ku Shaari, K.Z. and Abdullah, M.Z., 2013. Mesh sensitivity analysis of 3-dimensional microchannel for hydrodynamics simulation of one step urea synthesis.
- [24] Martic, I., Degiuli, N., Farkas, A. and Basic, J., 2017, June. Mesh Sensitivity Analysis for the Numerical Simulation of a Damaged Ship Model. In *ISOPE International Ocean and Polar Engineering Conference* (pp. ISOPE-I). ISOPE.
- [25] Mikulec, M. and Piehl, H., 2023. Verification and validation of CFD simulations with full-scale ship speed/power trial data. *Brodogradnja: Teorija i praksa brodogradnje i pomorske tehnike*, 74(1), pp. 41-62.
- [26] Kothari, C.R., 2004. *Research methodology: Methods and techniques*. New Age International.